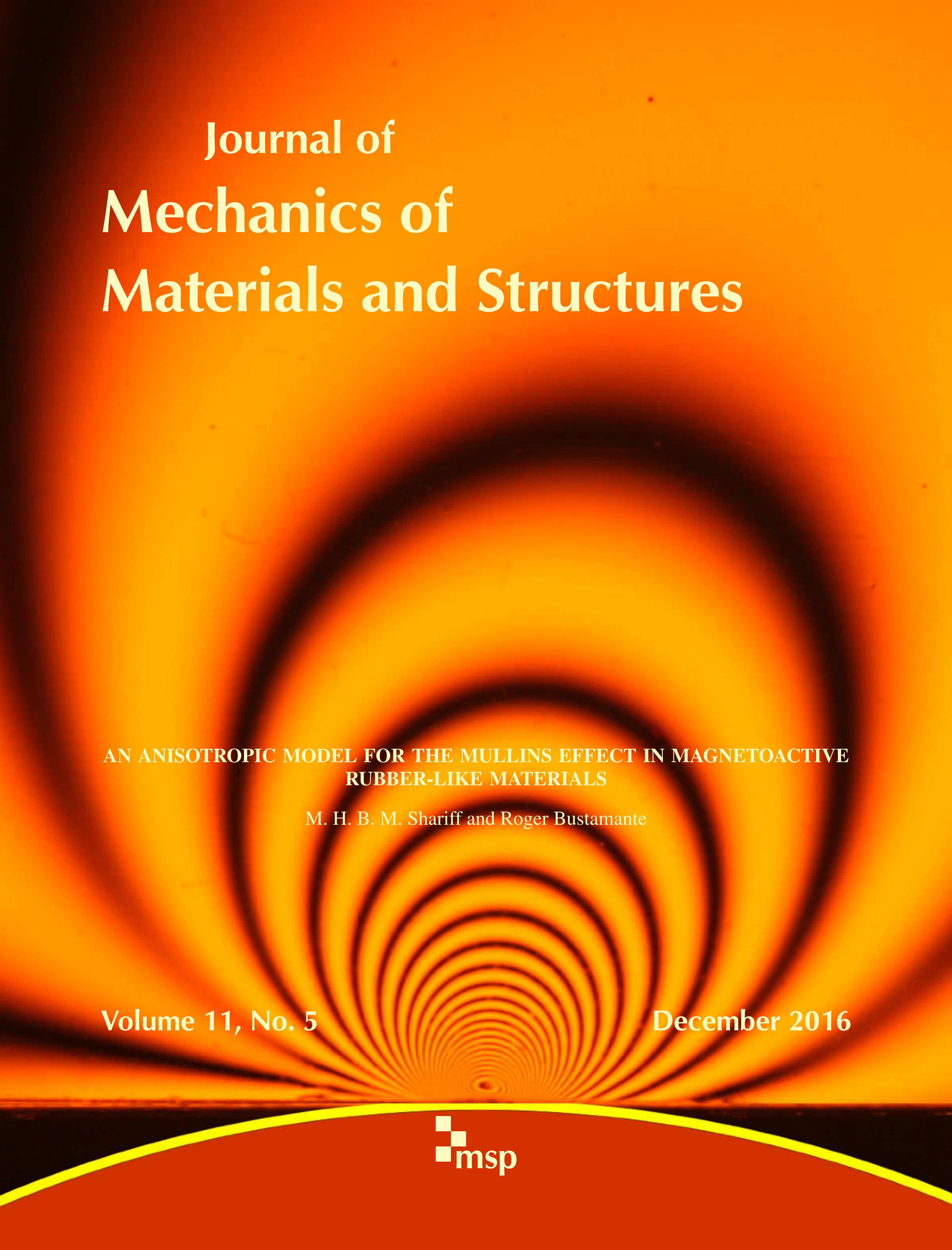

Journal of
Mechanics of
Materials and Structures

AN ANISOTROPIC MODEL FOR THE MULLINS EFFECT IN MAGNETOACTIVE RUBBER-LIKE MATERIALS

M. H. B. M. Shariff and Roger Bustamante

Volume 11, No. 5 December 2016

msp

JOURNAL OF MECHANICS OF MATERIALS AND STRUCTURES
Vol. 11, No. 5, 2016
dx.doi.org/10.2140/jomms.2016.11.559

AN ANISOTROPIC MODEL FOR THE MULLINS EFFECT IN MAGNETOACTIVE RUBBER-LIKE MATERIALS

M. H. B. M. SHARIFF AND ROGER BUSTAMANTE

An anisotropic phenomenological model is proposed to describe the Mullins phenomena for magnetoactive elastomers. The model is based on the use of direction-dependent damage parameters and a set of spectral invariants presented recently in the literature. The effect of the magnetic field on the Mullins phenomena for simple tension and simple shear is discussed.

1. Introduction

Magnetosensitive (MS) elastomers correspond to a class of rubber-like materials, which are filled with magnetoactive particles during the curing process, where the particles are usually made of iron and carbonyl iron (see, for example, [Bellan and Bossis 2002; Boczkowska and Awietjan 2012]). When such an elastomer solidifies, the MS particles remain locked inside it. Subsequently, if an external magnetic field is applied, it is possible to obtain relatively large deformations [Bellan and Bossis 2002; Boczkowska and Awietjan 2012] that can be controlled by this external field, and for this reason this class of elastomers is classified as a smart material [Ginder et al. 2001; Ghafoorianfar et al. 2013]. There are many possible applications for these elastomers, such as in the design of flexible robots and in vibration suppression [Böse et al. 2012; Farshad and Roux 2004; Kashima et al. 2012; Zhu et al. 2012].

Due to the potential applications of these MS elastomers, in the last few years there has been an interest in the mathematical modeling of the mechanical behavior of such materials. Some relatively recent works on this topic are the series of papers by Dorfmann and Ogden [2003; 2004a; 2004b; 2005], Triantafyllidis and coworkers [Kankanala and Triantafyllidis 2004; Danas et al. 2012], Steigmann [2004] and Vu and Steinmann [2010][1].

In most of these works, the MS elastomers were assumed to be hyperelastic bodies; however, when mixing a rubber-like material with MS particles, we expect to observe some inelastic phenomena since most elastomers, especially elastomers with fillers, exhibit an anisotropic stress-softening phenomenon widely known as the Mullins effect [Mullins 1947; Coquelle and Bossis 2006]. Quite often, the stress is softened significantly, hence modeling MS elastomers as purely elastic deformations can be erroneous. In addition to this, modeling the nonvirgin reference stress-free state of an MS material as isotropic is not accurate, since generally it is not isotropic in the stress-free reference state and the type of anisotropy depends on the history of strain.

Keywords: magnetoactive materials, Mullins effect, anisotropic stress-softening, spectral invariants.

[1] See the book by Ogden and Steigmann [2010] for more references on this topic; the interested reader can also see [Brown 1966; Eringen and Maugin 1990; Maugin 1988] for some older works on the interaction of electromagnetic fields and continua.

In the present communication, the mechanical behavior of MS elastomers is modeled via an anisotropic Mullins model, which is based on the direction-dependent model proposed by Shariff [2014]. In particular, we are interested in studying the influence of the magnetic field on the anisotropic stress softening behavior of MS elastomers, where we currently believe there is no model that could describe three-dimensional anisotropic stress-softening behavior (Mullins effect) of MS materials in the presence of a magnetic field. Our proposed model is based on the model of Shariff [2014], where he uses direction-dependent damage parameters (that depend on the history of strain) to simulate the anisotropic behavior that manifests due to the Mullins effect. His model is able to reasonably predict a variety of nonproportional (i.e., successive loadings with different directions of stretching or types of loading) experimental data on the anisotropic Mullins effect for different types of rubber-like materials. The constitutive equations for MS elastomers proposed in the present paper are characterized using a set of (useful) experimentally spectral invariants recently developed in the literature by Shariff and coworkers [Bustamante and Shariff 2015; Shariff 2008]. Most MS elastomers are nearly incompressible, however, in this communication it is assumed, for simplicity, that they are incompressible.

This paper is divided in the following parts: in Section 2 the main elements of the theory of Dorfmann and Ogden [2003; 2004b; 2004a; 2005] for MS elastomers are presented. In Section 3 the model for the Mullins effect is shown, while in Section 4 some boundary value problems are studied. Finally, in Section 5 some final comments are given.

2. Preliminary

2.1. *Kinematics.* In this paper, all subscripts i, j and k take the values 1, 2, 3, unless stated otherwise.

Let $\mathcal{B}$ denote the MS body, and $\boldsymbol{x} \in \mathcal{B}_t$ denote the position of a particle $X \in \mathcal{B}$ in the current configuration $\mathcal{B}_t$. The position of the same particle in the reference configuration is denoted as $\boldsymbol{X} \in \mathcal{B}_r$, where $\mathcal{B}_r$ is the body in the reference configuration, which is assumed to be undeformed and unstressed. It is assumed that there exists a one-to-one mapping $\boldsymbol{\chi}$ such that $\boldsymbol{x} = \boldsymbol{\chi}(\boldsymbol{X}, t)$ for any time $t > 0$. The deformation gradient, the left Cauchy–Green $\boldsymbol{B}$ and right Cauchy–Green $\boldsymbol{C}$ deformation tensors are respectively defined as

$$\boldsymbol{F} = \frac{\partial \boldsymbol{x}}{\partial \boldsymbol{X}}, \quad \boldsymbol{B} = \boldsymbol{F}\boldsymbol{F}^{\mathrm{T}} = \boldsymbol{V}^2, \quad \boldsymbol{C} = \boldsymbol{F}^{\mathrm{T}}\boldsymbol{F} = \boldsymbol{U}^2, \tag{1}$$

where $\boldsymbol{\chi}$ is assumed such that $J = \det \boldsymbol{F} > 0$.

In this communication, only quasistatic deformations and time-independent fields are considered, and the mechanical body forces are assumed to be negligible.

2.2. *Governing equations for magnetosensitive elastomers.*

2.2.1. *The Maxwell equations.* The theory of magnetosensitive elastomers (with no dependence on time) employed here makes use of three vector fields in the current configuration — the magnetic field $\boldsymbol{h}$, the induction $\boldsymbol{b}$ and the magnetic polarization $\boldsymbol{m}$ — to describe the magnetic effects in an MS body. In the absence of electric interactions and time effects, the magnetic field and the magnetic induction have to satisfy the simplified form of the Maxwell equations

$$\operatorname{div} \boldsymbol{b} = 0, \quad \operatorname{curl} \boldsymbol{h} = \boldsymbol{0}, \tag{2}$$

where, respectively, div and curl are the divergence and curl operators with respect to $\boldsymbol{x}$. Using the global form of (2), it is possible to define the following Lagrangian counterparts (in the reference configuration) of the magnetic field $\boldsymbol{h}_l$, and the magnetic induction $\boldsymbol{b}_l$

$$\boldsymbol{h}_l = \boldsymbol{F}^T \boldsymbol{h}, \quad \boldsymbol{b}_l = \boldsymbol{F}^{-1} \boldsymbol{b}. \tag{3}$$

The above variables satisfy [Dorfmann and Ogden 2004a]

$$\operatorname{Div} \boldsymbol{b}_l = 0, \quad \operatorname{Curl} \boldsymbol{h}_l = \boldsymbol{0}, \tag{4}$$

where Div and Curl are the divergence and curl operators with respect to $\boldsymbol{X}$, respectively.

In vacuum, the magnetic field and the magnetic induction are related by the equation

$$\boldsymbol{b} = \mu_0 \boldsymbol{h}, \tag{5}$$

where μ_0 is the magnetic permeability in vacuo. For condensed matter, an additional field is required, which is the magnetization field $\boldsymbol{m}$ and it is related to $\boldsymbol{b}$ and $\boldsymbol{h}$ through (see [Kovetz 2000] for more details on the theory of electromagnetism)

$$\boldsymbol{b} = \mu_0(\boldsymbol{h} + \boldsymbol{m}). \tag{6}$$

2.2.2. *The theory of magnetoelastic interactions by Dorfmann and Ogden .* In nonlinear magnetoelasticity, there are different ways to express the equation of motion, the relation between the stresses, the strains and the magnetic variables; there are also different possible definitions for the stress tensor [Hutter et al. 2006]. In this communication, as a basis for our work the theory developed by Dorfmann and Ogden [2004a] is used, where they define a total stress tensor $\boldsymbol{T}$ that incorporates in its definition the magnetic body forces (which are expressed as the divergence of a Maxwell stress tensor). The total (symmetrical) stress tensor $\boldsymbol{T}$ is related to the nonsymmetrical (elastic) Cauchy $\boldsymbol{\sigma}$ stress via the relation [Dorfmann and Ogden 2004b]

$$\boldsymbol{T} = \boldsymbol{\sigma} + \frac{1}{\mu_0}\big[\boldsymbol{b} \otimes \boldsymbol{b} - \tfrac{1}{2}(\boldsymbol{b} \cdot \boldsymbol{b})\boldsymbol{I}\big] + (\boldsymbol{m} \cdot \boldsymbol{b})\boldsymbol{I} - \boldsymbol{b} \otimes \boldsymbol{m}, \tag{7}$$

where $\otimes$ and $\cdot$ denote the dyadic and dot products, respectively. The nonsymmetrical mechanical Cauchy stress $\boldsymbol{\sigma}$ is part of the symmetrical total stress, and its role is important in deriving the proposed total energy (see (16) below). A key ingredient of this theory is the definition of a total energy function (see [Dorfmann and Ogden 2004a, Equation 3.10] and Section 3.3 below), where relatively simple expressions for the total stress and one of the magnetic variables are obtained.

2.2.3. *Equation of equilibrium and continuity conditions.* The total stress tensor $\boldsymbol{T}$ must satisfy the balance equation [Dorfmann and Ogden 2004a, Equation 2.13]

$$\operatorname{div} \boldsymbol{T} = \boldsymbol{0}. \tag{8}$$

Through the surface of the body $\partial\mathcal{B}_t$ the magnetic variables and the total stress tensor must satisfy the continuity conditions [Kovetz 2000]

$$\boldsymbol{n} \cdot [\![\boldsymbol{b}]\!] = 0, \quad \boldsymbol{n} \times [\![\boldsymbol{h}]\!] = \boldsymbol{0}, \quad \boldsymbol{T}\boldsymbol{n} = \hat{\boldsymbol{t}} + \boldsymbol{T}_M \boldsymbol{n}, \tag{9}$$

where $\boldsymbol{n}$ is the unit outward normal vector to $\partial\mathcal{B}_t$, $\hat{\boldsymbol{t}}$ is the external mechanical traction, $[\![\ ]\!]$ denotes the difference of a quantity from outside and inside a body, and $\boldsymbol{T}_m$ is the Maxwell stress tensor with the relation [Kovetz 2000]

$$\boldsymbol{T}_M = \boldsymbol{h} \otimes \boldsymbol{b} - \tfrac{1}{2}(\boldsymbol{h} \cdot \boldsymbol{b})\boldsymbol{I}. \tag{10}$$

3. Anisotropic stress softening model

When rubber is loaded in simple tension from its virgin state, and is then unloaded and reloaded, due to some damage, the stress required is less than that of the initial loading for stretches up to the maximum stretch achieved on the initial loading. This stress softening phenomenon is referred to as the Mullins effect. Here, a brief description on the behavior of the ideal Mullins effect is given; the unloading and reloading (in the same direction and up to the same "maximal" strain) paths coincide, and there is no permanent set. This description is made clear in Figure 1 below. In this section, we also define direction-dependent damage parameters, introduce the concept of the damage function [Shariff 2006; 2014] and construct a total energy function using a set of spectral invariants. In this communication, the term "damage" is interpreted in its widest sense; for example, it may mean "rupture of molecular bonds that reform to create new microstructure" or "conversion of hard phase to soft phase" or "any change in the ground state mechanical properties that are induced by strain". We are only concerned with strain induced damages that lead to stress softening.

3.1. ***Description of the ideal Mullins effect in nonproportional uniaxial loadings with no permanent set.*** Consider the case when there is no magnetic field ($h = 0$) and a magnetosensitive (MS) material is being prestretched uniaxially as shown on the primary (virgin material response) loading path Oa in Figure 1. On unloading from a the *elastic* path aEO is followed; we call this path elastic because when the material is loaded again up to point a the path aEO is retraced as OEa, hence the material behaves elastically and its ground-state-material-constant values are fixed during this deformation. From the point a the material is loaded to the point b via the primary loading path Oab. When the material is unloaded from b, the elastic bEO path is followed. After unloading completely, a simple tension deformation is applied in a direction 30° from the prestretch loading direction on a smaller specimen cut

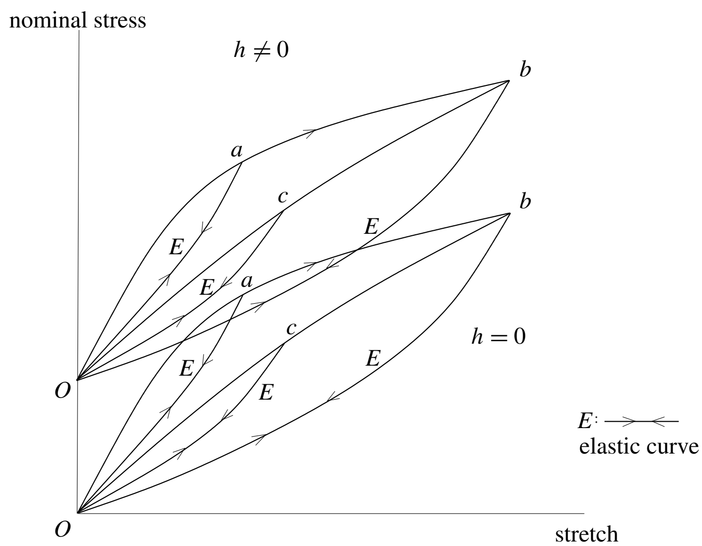

Figure 1. Schematic loading-unloading curves in simple tension of an MS Mullins material.

from the prestretched material. This sequence of deformations was done experimentally by Machado et al. [2012] on a non-MS material. The nonelastic 30° path is depicted by the path Ocb and the elastic paths (unloading from c and b) are depicted by cEO and bEO. The elastic properties for the elastic paths OEa, OEb and OEc are different. The nominal stress on any path can be obtained by differentiating the area under an elastic path. From Figure 1, the stress-strain behavior in different loading directions are not the same, which suggests that the damage caused by strain is anisotropic. The areas under different elastic paths can be represented by different direction dependent total elastic energy functions, although the material itself is not elastic. Note that the ground state material properties may change during deformation. With these in mind, following the work of Shariff [2006; 2014], we introduce a "free" energy function for an inelastic solid that can be portrayed by an infinite family of total elastic energy functions parameterized by the direction-dependent damage parameter defined in Section 3.2.

When a magnetic field ($h \neq 0$) is applied on the undeformed reference configuration, the material will deform due to the magnetic forces. In this case, an external stress is required to maintain that undeformed configuration $\boldsymbol{F} = \boldsymbol{I}$. Consider the sequence of uniaxial deformations described previously, where the directions of the magnetic field are always in the uniaxial directions. The behavior of the loading paths are similar to the loading paths mentioned before, but due to the presence of a magnetic field the uniaxial stresses are generally higher (as depicted in Figure 1) than the stresses when there is no magnetic field [Bellan and Bossis 2002].

3.2. ***Direction-dependent damage parameter and damage function.*** Based on simple tension deformations, in the original work by Mullins [1947], it was assumed that stress softening takes place if the current (principle) tensile stretch is less than the maximum stretch. In view of this, most previous models [Mullins 1947; Govindjee and Simo 1991; Johnson and Beatty 1993; Itskov et al. 2010] used maximum tensile stretch as their damage parameter. However, in simple tension there are three principal stretches, one in tension and two in compression; hence one should consider both the maximum tensile and minimum compressive stretches. It is worth noting that the Pawelski [2001] experiment showed that stress softening also occurs in compression. This suggests that minimum compressive stretch should not be ignored in stress softening modeling and hence, in our model, we include both the maximum and minimum stretches. They are related to the proposed direction-dependent damage parameter α_i as explained below.

The principal stretches satisfy the following inequality

$$s_i^{(\min)} \leq \lambda_i \leq s_i^{(\max)}, \tag{11}$$

where

$$s_i^{(\max)} = \max_{0 \leq z \leq t} \sqrt{\boldsymbol{e}_i \cdot \boldsymbol{C}(z)\boldsymbol{e}_i} \quad \text{and} \quad s_i^{(\min)} = \min_{0 \leq z \leq t} \sqrt{\boldsymbol{e}_i \cdot \boldsymbol{C}(z)\boldsymbol{e}_i}. \tag{12}$$

Physically, $s_i^{(\max)}$ and $s_i^{(\min)}$ are the maximum and minimum "stretch" values of the $\boldsymbol{e}_i$ line element throughout the history of the deformation, respectively. From the above equation it is clear that $s_i^{(\max)} \geq 1$, $s_i^{(\min)} \leq 1$ and λ_i is bounded by $s_i^{(\min)}$ and $s_i^{(\max)}$. Consider, for example, a material being prestretched by a simple tension deformation process. A simple tension deformation is then applied on this prestretch material in the same direction as the prestretch direction, where the deformation is described by

$$\boldsymbol{U}(\lambda) \equiv \big(\lambda, 1/\sqrt{\lambda}, 1/\sqrt{\lambda}\big), \tag{13}$$

where $1 \le \lambda \le \lambda_m = s_1^{(\max)}$, $s_2^{(\min)} = s_3^{(\min)} = 1/\sqrt{\lambda_m} \le 1/\sqrt{\lambda} \le 1$ and $s_1^{(\min)} = s_2^{(\max)} = s_3^{(\max)} = 1$. In (12), $s_i^{(\max)}$ and $s_i^{(\min)}$ are related to the amount of damage; the interval in (11) widens as the amount of damage increases.

For a non-MS Mullins material, Shariff [2006; 2014] proposed an anisotropic stress softening damage model using the direction-dependent damage parameter α_i, where

$$\alpha_i = \begin{cases} s_i^{(\max)} & \text{when } \lambda_i > 1, \\ s_i^{(\min)} & \text{when } \lambda_i < 1. \end{cases} \tag{14}$$

Note that in (14) we do not consider $\lambda_i = 1$, because our model is constructed in such a way that α_i does not contribute to the stress softening when $\lambda_i = 1$ (see Section 3.5 below). In the case when $\lambda_i = \lambda_j$ ($i \ne j$), the directions of $\boldsymbol{e}_i$ and $\boldsymbol{e}_j$ are not unique. In view of this, we let

$$\alpha_i = \alpha_j = \begin{cases} 1/\sqrt{s_k^{(\min)}} & \text{when } \lambda_i = \lambda_j > 1, \\ 1/\sqrt{s_k^{(\max)}} & \text{when } \lambda_i = \lambda_j < 1, \end{cases} \tag{15}$$

where $i \ne j \ne k \ne i$. In the case when all the principal stretches are equal, the principal directions $\boldsymbol{e}_i$ are all nonunique. However, for an incompressible material this can only happen when $\lambda_1 = \lambda_2 = \lambda_3 = 1$ and, as mentioned above, the corresponding α_i in this case do not contribute to the stress softening; hence their values are not given here.

Stress softening models usually have softening functions which control the softening behavior. The softening function is governed by the amount of damage [Simo 1987; Ogden and Roxburgh 1999; Itskov et al. 2010]. The rate of change of the amount of damage with respect to time or any deformation parameter that increases with primary loading should be nonnegative. In our model, in view of the definition of the damage parameter α_i, a measure of an amount of damage (damage function) related to the $\boldsymbol{e}_i$ line element is proposed. The proposed damage function g (which may depend on material properties) is defined such that $0 = g(1) \le g(x)$, $x \in R$, $x > 0$. The function g has also the properties that $\hat{g}'(\alpha) \ge 0$, where $\hat{g}(\alpha) = g((1-\alpha) + \alpha w)$, $0 < \alpha \le 1$ and $w > 0\,(\ne 1)$ is a constant. The function $\hat{g}'(\alpha)$ need not be defined at $\alpha = 0$. If it is defined then $\hat{g}'(0) = 0$. In view of our definition, g increases monotonically as x moves away from the point $x = 1$; hence, $g(\lambda_i) \le g(\alpha_i)$. Physically, $g(\alpha_i)$ can be considered as a measure of an amount of damage related to the $\boldsymbol{e}_i$ line element; for a strictly monotonic g, the higher the value of g the bigger the damage induced on the $\boldsymbol{e}_i$ line element. Specific forms of g are given below in (64) and (72).

3.3. ***Constitutive equations and spectral invariants .*** For an isothermal problem the Clausius–Duhem inequality take the form

$$\boldsymbol{\sigma} : \boldsymbol{D} - \rho_0 \dot{\psi} - \boldsymbol{m} \cdot \dot{\boldsymbol{b}} \ge 0, \tag{16}$$

where the superposed dot represents the time derivative, : denotes the inner product of two second order tensors, ρ_0 is the density of the incompressible material, ψ is the Helmholtz free energy function, $\boldsymbol{D} = \operatorname{grad} \boldsymbol{v}$, grad is the gradient operator with respect to $\boldsymbol{x}$ and $\boldsymbol{v}$ is the velocity. Following [Dorfmann and Ogden 2004a] and [Shariff 2014] the Helmholtz free energy can be expressed as

$$\rho_0 \psi = \psi_a(\boldsymbol{F}, \boldsymbol{b}, \boldsymbol{g}), \tag{17}$$

where the vector $\boldsymbol{g} \equiv [g(\alpha_1), g(\alpha_2), g(\alpha_3)]^T$ is an internal variable. Taking note that, for an incompressible material $\mathrm{tr}(\boldsymbol{D}) = 0$, and since $\boldsymbol{\sigma} : \boldsymbol{D} = (\boldsymbol{F}^{-1}\boldsymbol{\sigma})^T : \dot{\boldsymbol{F}}$, (16) and (17) give the relations

$$\left(\boldsymbol{\sigma} + p\boldsymbol{I} - \boldsymbol{F}\frac{\partial \psi_a}{\partial \boldsymbol{F}}\right) : \dot{\boldsymbol{F}} - \left(\boldsymbol{m} + \frac{\partial \psi_a}{\partial \boldsymbol{b}}\right) \cdot \dot{\boldsymbol{b}} - \sum_{i=1}^{3} \frac{\partial \psi_a}{\partial g(\alpha_i)} \dot{g}(\alpha_i) \geq 0, \tag{18}$$

$$\boldsymbol{\sigma} = -p\boldsymbol{I} + \boldsymbol{F}\frac{\partial \psi_a}{\partial \boldsymbol{F}}, \quad \boldsymbol{m} = -\frac{\partial \psi_a}{\partial \boldsymbol{b}}, \tag{19}$$

and the inequality

$$-\sum_{i=1}^{3} \frac{\partial \psi_a}{\partial g(\alpha_i)} \dot{g}(\alpha_i) \geq 0\,. \tag{20}$$

In view of the property of g, $\dot{g}(\alpha_i) \geq 0$, and to satisfy (20), the condition

$$\frac{\partial \psi_a}{\partial g(\alpha_i)} \leq 0 \tag{21}$$

is imposed. If we define

$$\Phi(\boldsymbol{F}, \boldsymbol{b}_l, \boldsymbol{g}) = \psi_a(\boldsymbol{F}, \boldsymbol{F}\boldsymbol{b}_l, \boldsymbol{g}), \tag{22}$$

the nonsymmetric Cauchy stress [Dorfmann and Ogden 2004a] takes the form

$$\boldsymbol{\sigma} = -p\boldsymbol{I} + \boldsymbol{F}\frac{\partial \Phi}{\partial \boldsymbol{F}} - (\boldsymbol{m} \cdot \boldsymbol{b})\boldsymbol{I} + \boldsymbol{b} \otimes \boldsymbol{m}, \tag{23}$$

where p is the associated Lagrange multiplier due to the incompressibility constraint and $\boldsymbol{I}$ is the second order identity tensor.

Following [Dorfmann and Ogden 2004a], an amended free energy function

$$\Omega_m(\boldsymbol{F}, \boldsymbol{b}_l, \boldsymbol{g}) = \Phi(\boldsymbol{F}, \boldsymbol{b}_l, \boldsymbol{g}) + \frac{1}{2\mu_0}\boldsymbol{b}_l \cdot \boldsymbol{C}\boldsymbol{b}_l \tag{24}$$

is defined and using (24) the simplified relation

$$\boldsymbol{h}_l = \frac{\partial \Omega_m}{\partial \boldsymbol{b}_l} \tag{25}$$

is obtained.

In this paper, $\boldsymbol{h}_l$ is chosen (instead of $\boldsymbol{b}_l$) as the independent variable and a complementary (total) energy function $\Omega_e = \Omega_a(\boldsymbol{F}, \boldsymbol{h}_l)$ is defined through the partial Legendre transformation as

$$\Omega_e = \Omega_a(\boldsymbol{F}, \boldsymbol{h}_l, \boldsymbol{g}) = \Omega_m(\boldsymbol{F}, \boldsymbol{b}_l, \boldsymbol{g}) - \boldsymbol{b}_l \cdot \boldsymbol{h}_l, \tag{26}$$

where, in view of the inequality (21), the inequality

$$\frac{\partial \Omega_e}{\partial g(\alpha_i)} \leq 0 \tag{27}$$

is automatically satisfied. The relation

$$\boldsymbol{b}_l = -\frac{\partial \Omega_e}{\partial \boldsymbol{h}_l} \tag{28}$$

is obtained from (26).

If Ω_e is treated as a function of $\boldsymbol{C}$, the objectivity condition is automatically satisfied and can be written as

$$\Omega_e = \Omega_c(\boldsymbol{C}, \boldsymbol{a}, \boldsymbol{g}, h) = \Omega_a(\boldsymbol{F}, \boldsymbol{h}_l, \boldsymbol{g}), \tag{29}$$

where the unit vector $\boldsymbol{a} = \boldsymbol{h}_l / h$ and $h = |\boldsymbol{h}_l|$. Following the work of Spencer [1971], Ω_e can be expressed in terms classical invariants, i.e.,

$$\Omega_e = \Omega_d(I_1, I_2, I_4, I_5, \boldsymbol{g}, h), \tag{30}$$

where

$$I_1 = \mathrm{tr}(\boldsymbol{C}), \quad I_2 = \frac{I_1^2 - \mathrm{tr}(\boldsymbol{C}^2)}{2}, \quad I_4 = \boldsymbol{a} \cdot \boldsymbol{C}\boldsymbol{a}, \quad I_5 = \boldsymbol{a} \cdot \boldsymbol{C}^2\boldsymbol{a} \tag{31}$$

and tr denotes the trace of a second order tensor. Except for I_4, the rest of the above classical invariants have no immediate physical interpretation. Hence, they are not attractive in seeking to design a rational program of experiments[2] for MS solids. For example, it is not straightforward to design an experiment to construct (rigorously) a specific functional form of the total energy Ω_e, where the experiment requires varying a single classical invariant while keeping the remaining classical invariants fixed [Holzapfel and Ogden 2009; Humphrey et al. 1990; Lin and Yin 1998]. In this paper our total energy function is characterized using a set of spectral invariants, where each invariant has a clear physical meaning and have an experimental advantage [Shariff 2008] over the standard (classical and its variants) invariants commonly used in dealing with anisotropic problems. Note that

$$\boldsymbol{C} = \sum_{i=1}^{3} \lambda_i^2 \boldsymbol{e}_i \otimes \boldsymbol{e}_i, \tag{32}$$

where λ_i is a principal value (stretch) of the right stretch tensor $\boldsymbol{U}$, and $\boldsymbol{e}_i$ is a principal direction of $\boldsymbol{U}$. In view of (29) and (32),

$$\Omega_e = \Omega_f(\lambda_1, \lambda_2, \lambda_3, \boldsymbol{e}_1 \otimes \boldsymbol{e}_1, \boldsymbol{e}_2 \otimes \boldsymbol{e}_2, \boldsymbol{e}_3 \otimes \boldsymbol{e}_3, \boldsymbol{a}, \boldsymbol{g}, h). \tag{33}$$

Hence, following the work presented in [Shariff 2008], Ω_e can be written in terms of h and the corresponding spectral invariants, i.e.,

$$\Omega_e = \Omega(\lambda_1, \lambda_2, \lambda_3, \zeta_1, \zeta_2, \zeta_3, \boldsymbol{g}, h), \tag{34}$$

where $\zeta_i = (\boldsymbol{a} \cdot \boldsymbol{e}_i)^2$. The physical meaning of λ_i is obvious, and it is clear that ζ_i is the square of the cosine of the angle between the principal direction $\boldsymbol{e}_i$ and the preferred direction $\boldsymbol{a}$. Since $\boldsymbol{a}$ is a unit vector, this implies $\zeta_3 = 1 - \zeta_1 - \zeta_2$. The invariant h and the spectral invariants have an experimental advantage over classical invariants presented in the literature, e.g., a simple triaxial test can vary a single invariant while keeping the remaining invariants fixed [Shariff 2008].

Note that (34) has the symmetrical property

$$\Omega(\lambda_1, \lambda_2, \lambda_3, \zeta_1, \zeta_2, \zeta_3, \boldsymbol{g}, h) = \Omega(\lambda_2, \lambda_1, \lambda_3, \zeta_2, \zeta_1, \zeta_3, \boldsymbol{g}, h) = \Omega(\lambda_3, \lambda_2, \lambda_1, \zeta_3, \zeta_2, \zeta_1, \boldsymbol{g}, h). \tag{35}$$

[2] See [Criscione 2003] for a criticism on the use of the classical invariants by Spencer and Rivlin [1962].

In view of the nonunique values of $\boldsymbol{e}_i$ and $\boldsymbol{e}_j$ when $\lambda_i = \lambda_j$, a unique valued Ω should be independent of ζ_i and ζ_j when $\lambda_i = \lambda_j$ and Ω should be independent of ζ_1, ζ_2 and ζ_3 when $\lambda_1 = \lambda_2 = \lambda_3$. We call this independent property together with the symmetrical property (35) the P-property [Shariff 2016]. Our total energy function proposed later in this paper is required to satisfy the P-property.

In view of (22), (23), (24), (26) and (7),

$$\boldsymbol{T} = 2\boldsymbol{F}\frac{\partial \Omega_e}{\partial \boldsymbol{C}}\boldsymbol{F}^T - p\boldsymbol{I}. \tag{36}$$

The total nominal stress $\boldsymbol{S}$ is given by [Dorfmann and Ogden 2004b]

$$\boldsymbol{S} = \boldsymbol{F}^{-1}\boldsymbol{T}. \tag{37}$$

Following the results presented in [Shariff 2008], the Lagrangean spectral components of $\frac{\partial \Omega_e}{\partial \boldsymbol{C}}$ can be expressed as

$$\left(\frac{\partial \Omega_e}{\partial \boldsymbol{C}}\right)_{ii} = \frac{1}{2\lambda_i}\frac{\partial \Omega}{\partial \lambda_i} \quad (i \text{ not summed}), \tag{38}$$

and the shear components

$$\left(\frac{\partial \Omega_e}{\partial \boldsymbol{C}}\right)_{ij} = \frac{\boldsymbol{e}_i \cdot \boldsymbol{A}\boldsymbol{e}_j}{(\lambda_i^2 - \lambda_j^2)}\left(\frac{\partial \Omega}{\partial \zeta_i} - \frac{\partial \Omega}{\partial \zeta_j}\right), \tag{39}$$

where $\boldsymbol{A} = \boldsymbol{a} \otimes \boldsymbol{a}$. The Eulerian spectral components of T_{ij} of the total stress $\boldsymbol{T}$ are [Bustamante and Shariff 2015]

$$T_{ii} = \lambda_i \frac{\partial \Omega}{\partial \lambda_i} - p, \tag{40}$$

$$T_{ij} = 2\lambda_i\lambda_j \frac{\boldsymbol{e}_i \cdot \boldsymbol{A}\boldsymbol{e}_j}{(\lambda_i^2 - \lambda_j^2)}\left(\frac{\partial \Omega}{\partial \zeta_i} - \frac{\partial \Omega}{\partial \zeta_j}\right), \quad i \neq j. \tag{41}$$

Expressed in terms of spectral components, the magnetic induction has the form [Bustamante and Shariff 2015]

$$\boldsymbol{b}_l = \sum_{k=1}^{3} b_k \boldsymbol{e}_k, \tag{42}$$

where in view of (28)

$$b_k = -(\boldsymbol{a} \cdot \boldsymbol{e}_k)\left[\frac{\partial \Omega}{\partial h} + \frac{2}{h}\left(\frac{\partial \Omega}{\partial \zeta_k} - \sum_{i=1}^{3}\frac{\partial \Omega}{\partial \zeta_i}\zeta_i\right)\right]. \tag{43}$$

The magnetic induction in the deformed configuration is obtained from (3), i.e.,

$$\boldsymbol{b} = \boldsymbol{F}\boldsymbol{b}_l. \tag{44}$$

The Eulerian expression of $\boldsymbol{b}$ is simply

$$\boldsymbol{b} = \sum_{k=1}^{3} \lambda_k b_k \boldsymbol{v}_k, \tag{45}$$

where $\boldsymbol{v}_k$ is the principal direction of the left stretch tensor $\boldsymbol{V}$.

3.4. ***The undeformed configuration.*** Magnetic fields distort an MS body, so if the body is to remain in the undeformed state ($\boldsymbol{F} = \boldsymbol{I}$) when a magnetic field is applied, then it must be subject to an external traction that depends on the magnetic field. In the undeformed state, $\lambda_1 = \lambda_2 = \lambda_3 = 1$ and the principal directions of $\boldsymbol{U}$ are not unique. For simplicity, let $\boldsymbol{a} = \boldsymbol{e}_3$ such that $\zeta_3 = 1$, $\zeta_1 = \zeta_2 = 0$. From (40) and (41), for the case of when $\boldsymbol{h}_l$ is constant, it is necessary to apply an external traction such that the body remains undeformed, i.e.,

$$\boldsymbol{T} = \boldsymbol{T}_0 = \sum_{i=1}^{3} \frac{\partial \Omega}{\partial \lambda_i}(1, 1, 1, 0, 0, 1, h)\boldsymbol{e}_i \otimes \boldsymbol{e}_i - p\boldsymbol{I}. \tag{46}$$

From (42) and (43), the magnetic induction takes the form,

$$\boldsymbol{b} = -\Omega_0'(h)\boldsymbol{e}_3, \tag{47}$$

where

$$\Omega_0'(h) = \frac{\partial \Omega}{\partial h}(1, 1, 1, 0, 0, 1, h). \tag{48}$$

3.5. ***A specific constitutive equation.*** Using the damage parameter α_i and the above set of spectral invariants and following the work of [Bustamante and Shariff 2015; Shariff 2014], a simple separable constitutive equation

$$\Omega_e = \sum_{i=1}^{3} \big[\hat{\eta}(g(\lambda_i), g(\alpha_i))r(\lambda_i) + \phi(\lambda_i, \alpha_i) + \zeta_i z(\lambda_i, h)\big] \tag{49}$$

$$= \sum_{i=1}^{3} \left[\int_1^{\lambda_i} \hat{\eta}(g(y), g(\alpha_i))r'(y)\,\mathrm{d}y + \zeta_i z(\lambda_i, h)\right] \tag{50}$$

is proposed, where

$$\phi(\lambda_i, \alpha_i) = -\int_1^{\lambda_i} r(y)\frac{\mathrm{d}\hat{\eta}}{\mathrm{d}y}(g(y), g(\alpha_i))\,\mathrm{d}y \tag{51}$$

and

$$z(y, h) = q(y, h) - \frac{\mu_0 h^2}{2y^2}. \tag{52}$$

The first term of the total energy Ω_e (50) can be considered as the sum of energies, where each energy depends on λ_i and on the damage function $g(\alpha_i)$ of the $\boldsymbol{e}_i$ line element, while the second term can be considered as the sum of energies, where each energy depends on λ_i, the magnitude of $\boldsymbol{h}$ and its components in the principal directions of $\boldsymbol{U}$. The Eulerian magnetic induction then takes the form

$$\boldsymbol{b} = -\boldsymbol{F}\frac{\partial Q}{\partial \boldsymbol{h}_l} + \mu_0 \boldsymbol{h} \tag{53}$$

and the magnetization is

$$\boldsymbol{m} = -\frac{\boldsymbol{F}}{\mu_0}\frac{\partial Q}{\partial \boldsymbol{h}_l}, \tag{54}$$

where

$$Q = \sum_{i=1}^{3} \zeta_i q(\lambda_i, h). \tag{55}$$

For simplicity of notation, let

$$\eta(y, d) = \hat{\eta}(g(y), g(d)). \tag{56}$$

The stress softening function η is introduced in (50) to soften the stress and has the properties $0 < \eta \leq 1$ and $\eta(s, s) = 1$. In view of (53), (54) and (55), it is clear that in vacuum $\boldsymbol{b} = \mu_0 \boldsymbol{h}$ and $\boldsymbol{m} = 0$, and our model suggests that the magnetic induction and the magnetization are independent of the stress-softening, although the stress is affected by the magnetic field and the softening function.

The free energy (50) satisfies the P-property and is direction dependent since the damage parameter α_i is direction-dependent and hence it describes anisotropic damage.

On the primary loading $\eta = 1$, the free energy function simply becomes

$$\Omega_e = \sum_{i=1}^{3} [r(\lambda_i) + \phi(\lambda_i, \alpha_i) + \zeta_i z(\lambda_i, h)]. \tag{57}$$

Based on the work of Shariff [2000] on nonlinear isotropic elasticity, we let

$$r(\lambda_i) = \int_1^{\lambda_i} \frac{f(y)}{y}\, \mathrm{d}y, \tag{58}$$

where $f(1) = 0$ and f is strictly monotone. It is clear that $r(1) = 0$, $r'(1) = 0$, $0 = r(1) \leq r(y)$ and $r(y)$ increases (strictly) monotonically away from $y = 1$.

The condition

$$\frac{\partial \hat{\eta}}{\partial g(\alpha_i)}(g(\lambda_i), g(\alpha_i)) < 0 \tag{59}$$

ensures that the inequality (27) is satisfied.

In this paper, we are not concerned with specific forms of the functions f, η, g and q, since there is no available experimental data in the literature about Mullins effect for MS elastomers. However, some qualitative properties of the functions f, η and g are discussed in [Shariff 2014] and specific forms for f, η and g can be found in [Shariff 2000; 2014], i.e.,

$$f(y) = \sum_{i=1}^{4} a_i \phi_i(y), \tag{60}$$

where

$$\phi_1(y) = \tfrac{2}{3} \ln(y), \quad \phi_2(y) = e^{(1-y)} + y - 2, \quad \phi_3(y) = e^{(y-1)} - y, \tag{61}$$

$$\phi_4(y) = \frac{(y-1)^3}{y^k}, \tag{62}$$

a_1, a_2, a_3, a_4 and k are material constants,

$$\hat{\eta}(g(y), g(d)) = e^{b_1 (g(y) - g(d)) g(y)^{b_2}} - b_3 e^{-b_4 g(y)} (g(d) - g(y)), \tag{63}$$

where b_1, b_2 and b_3 are material constants and

$$g(y) = \frac{(y^{c_1} - 1)^2}{y^{c_2}}, \tag{64}$$

where c_1 and c_2 are material constants and must be constrained so that $g(y)$ increases monotonically as y moves away from the point $y = 1$ [Shariff 2014]. In this paper we let

$$z(y, h) = d_1 \frac{\mu_0 h^2}{2y^2} - \frac{\mu_0 h^2}{2y^2}, \tag{65}$$

where d_1 is a material constant.

4. Homogeneous deformations

The objective of this section is to discuss the anisotropic mechanical behavior of the proposed constitutive model in simple tension and simple shear deformations, where it can be important from the experimental point of view. We note in passing, that for non-Mullins behavior, simple tension experiments have been done by Bellan and Bossis [2002] and a simple shear experiment has been done by Jolly et al. [1996]. Results for nonproportional loadings to analyze the anisotropic behavior of Mullins materials are given in this section. In the simple shear case, results on the anisotropic behavior due to the application of a magnetic field in different directions are also given.

4.1. *Simple tension.* Due to edge effects, the continuity conditions on the surfaces are not easily satisfied when simple tension is applied on a rectangular slab. To reduce the edge effects, a specific slab configuration is considered, where the slab thickness in the $\boldsymbol{e}_3$ direction is very small relative to its width (which is in the $\boldsymbol{e}_1$ direction), and its length in the $\boldsymbol{e}_2$ direction is very large relative to its width[3]. This configuration is denoted as the S-configuration. A simple tension is applied in the $\boldsymbol{e}_2$ direction.

4.1.1. *Simple tension in a fixed direction.* To discuss the effect of a magnetic field on stress-softening materials in fixed direction loadings, a simple tension in the Cartesian 2-direction is considered and the magnetic field $\boldsymbol{h}_l \equiv [0, h, 0]^T$ is applied (where h is a constant) in the undeformed configuration which automatically satisfies (4). With this particular type of deformation, the spectral variables take values $\zeta_2 = 1$, $\zeta_1 = \zeta_3 = 0$. Consider $1 \leq \lambda_2 = \lambda \leq \lambda_m$, hence $s_2^{(\max)} = \lambda_m$ and $s_3^{(\max)} = s_1^{(\max)} = 1/\sqrt{\lambda_m} = 1/\sqrt{s_2^{(\max)}}$. The total uniaxial stress simply takes the form

$$T_{22}(\lambda_2, h) = \eta(\lambda, s_2^{(\max)}) f(\lambda) - \eta\left(\frac{1}{\sqrt{\lambda}}, \frac{1}{\sqrt{s_2^{(\max)}}}\right) f\left(\frac{1}{\sqrt{\lambda}}\right) + \lambda \frac{\partial z}{\partial \lambda}(\lambda, h) - \mu_0 \frac{h^2}{2\lambda^2}. \tag{66}$$

The derivation of (66) has taken into account the effect of the Maxwell stress

$$T_{M_{33}} = -\mu_0 \frac{h^2}{2\lambda^2} \tag{67}$$

[3] It is assumed that the length in direction 2 is very large in comparison with the dimensions in the other two directions so that the continuity conditions (9) and (10) are satisfied only for the surface with normal $\boldsymbol{e}_3$.

at the exterior surfaces of the material, where it is assumed that there are no mechanical stresses at these surfaces. In the undeformed configuration,

$$T_{22}(1,h)=\frac{\partial z}{\partial \lambda}(1,h)-\mu_0\frac{h^2}{2}. \tag{68}$$

Without the magnetic field it is expected that $T_{22}(1,0)=0$ in the undeformed configuration. Hence, the condition $\frac{\partial z}{\partial \lambda}(1,0)=0$ is imposed. It is assumed that the magnetic induction and the magnetization are given as $\boldsymbol{b}\equiv[0,-\lambda(\frac{\partial z}{\partial h}(\lambda,h)),0]^T$ and $\boldsymbol{m}\equiv[0,m,0]^T$, where

$$m=-\frac{1}{\mu_0}\lambda\frac{\partial q}{\partial h}(\lambda,h). \tag{69}$$

In this section, for illustrative purposes, it is assumed

$$z(y,h)=\mu_0 h^2\left(\frac{d_1}{(y-a)^2+y}-\frac{1}{2y^2}\right) \tag{70}$$

which satisfies the property $\frac{\partial z}{\partial \lambda}(1,0)=0$ mentioned previously. For simplicity, consider [Shariff 2014]

$$\eta(y,d)=e^{b_1(g(y)-g(d))g(y)^{b_2}}, \tag{71}$$

$$g(y)=\frac{(y-1)^2}{y} \tag{72}$$

and

$$f(y)=a_1\phi_1(y)+a_2\phi_2(y), \tag{73}$$

with the ad hoc values

$$a=1.2,\quad a_1=a_2=1.0\,\text{kPa},\quad b_1=2,\quad b_2=0.5,\quad d_1=-2\,\text{kPa}$$

for the material constants.

In Figure 2, the nominal stress (T_{22}/λ_2)-strain behavior is depicted for $\lambda_m=2.5$, and from the figure it is clear that our model produces stiffer stress when a magnetic field is applied and stress softening Mullin's behavior is simulated. The behavior of the stress difference depicted in Figure 3 due to two different magnetic field values is similar to the experimental behavior found in Coquelle and Bossis [2006].

4.1.2. *Anisotropy induced by a uniaxial prestretch.* Here, uniaxial deformations of the nonvirgin MS material in directions different from the uniaxial prestretch direction are studied. Experiments on these types of deformations on a non-MS material have been done by Machado et al. [2012], and Shariff [2014] has developed a model to successfully describe these deformations. Consider a uniaxial prestretch deformation in the 2-direction (corresponds to 0°) of S-configuration virgin samples defined by

$$\boldsymbol{U}(\lambda)\equiv\operatorname{diag}(1/\sqrt{\lambda},\lambda,1/\sqrt{\lambda}), \tag{74}$$

where $1\le\lambda\le\lambda_m$.

Then a set of smaller S-configuration specimens is cut from each of these preconditioned large samples in different directions and each direction corresponds to an angle θ (the angle subtended, anticlockwise,

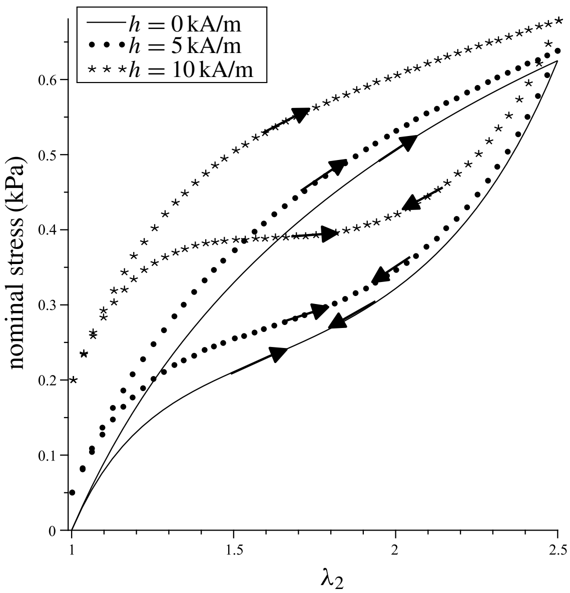

Figure 2. Simple tension in a fixed 2-direction for different magnetic field values.

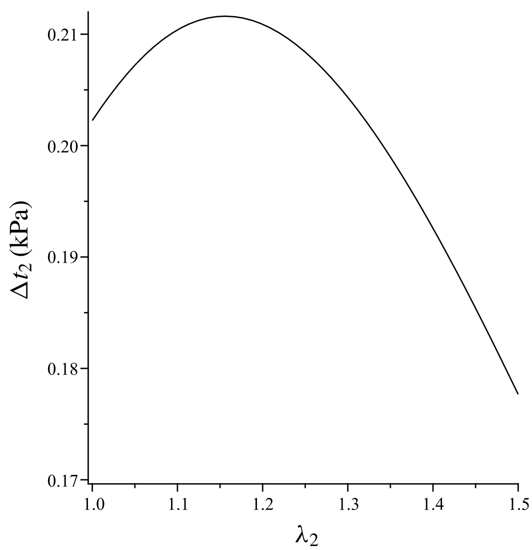

Figure 3. Simple tension in a fixed 2-direction, where $\lambda = \lambda_2$ and $\Delta t_2 = T_{22}/\lambda_2\,(\lambda, 10) - T_{22}/\lambda_2\,(\lambda, 0)$.

from the 2 direction). Each of these smaller specimens is then subjected to a uniaxial deformation in one of these directions and we let this direction to be the $\boldsymbol{e}_2$ direction, where the Cartesian components of the principal directions of $\boldsymbol{U}$ are given by

$$\boldsymbol{e}_1 \equiv \begin{bmatrix} c \\ s \\ 0 \end{bmatrix}, \quad \boldsymbol{e}_2 \equiv \begin{bmatrix} -s \\ c \\ 0 \end{bmatrix}, \quad \boldsymbol{e}_3 \equiv \begin{bmatrix} 0 \\ 0 \\ 1 \end{bmatrix}, \tag{75}$$

where $c = \cos(\theta)$, $s = \sin(\theta)$ and $0 \le \theta \le \pi/2$. Consider the extremum values

$$\hat{s}_i^{(\max)} = \max_{1 \le \lambda \le \lambda_m} \sqrt{\boldsymbol{e}_i \cdot \boldsymbol{U}^2(\lambda)\boldsymbol{e}_i}, \quad \hat{s}_i^{(\min)} = \min_{1 \le \lambda \le \lambda_m} \sqrt{\boldsymbol{e}_i \cdot \boldsymbol{U}^2(\lambda)\boldsymbol{e}_i} \tag{76}$$

of the prestretch deformation in the $\boldsymbol{e}_i$ directions. The extremum values given in (76) are [Shariff 2014]:

$$\hat{s}_1^{(\max)} = \begin{cases} 1, & 1 \ge c \ge \sqrt{\lambda_m(1+\lambda_m)/(1+\lambda_m+\lambda_m^2)}, \\ f_c(\lambda_m), & 0 \le c \le \sqrt{\lambda_m(1+\lambda_m)/(1+\lambda_m+\lambda_m^2)}, \end{cases} \tag{77}$$

$$\hat{s}_1^{(\min)} = \begin{cases} 1, & 0 \le c \le \sqrt{\frac{2}{3}}, \\ f_c\big(c^2/(2(1-c^2))\big)^{1/3}, & \sqrt{\frac{2}{3}} \le c \le \sqrt{2\lambda_m^3/(1+2\lambda_m^3)}, \\ f_c(\lambda_m), & \sqrt{2\lambda_m^3/(1+2\lambda_m^3)} \le c \le 1, \end{cases} \tag{78}$$

$$\hat{s}_2^{(\max)} = \begin{cases} 1, & 1 \ge s \ge \sqrt{(\lambda_m(1+\lambda_m))/(1+\lambda_m+\lambda_m^2)}, \\ f_s(\lambda_m), & 0 \le s \le \sqrt{(\lambda_m(1+\lambda_m))/(1+\lambda_m+\lambda_m^2)}, \end{cases} \tag{79}$$

$$\hat{s}_2^{(\min)} = \begin{cases} 1, & 0 \le s \le \sqrt{\frac{2}{3}}, \\ f_s\big(s^2/(2(1-s^2))\big)^{1/3}, & \sqrt{\frac{2}{3}} \le s \le \sqrt{2\lambda_m^3/(1+2\lambda_m^3)}, \\ f_s(\lambda_m), & \sqrt{2\lambda_m^3/(1+2\lambda_m^3)} \le s \le 1, \end{cases} \tag{80}$$

$$\hat{s}_3^{(\max)} = 1, \quad \hat{s}_3^{(\min)} = \frac{1}{\lambda_m}, \tag{81}$$

where

$$f_c(\lambda) = \sqrt{(1/\lambda - \lambda^2)c^2 + \lambda^2}, \quad f_s(\lambda) = \sqrt{(1/\lambda - \lambda^2)s^2 + \lambda^2}. \tag{82}$$

The maximum and minimum values for the principal-direction line elements corresponding to (75) during the deformation of the prestretch nonvirgin material are

$$s_i^{(\max)} = \begin{cases} \hat{s}_i^{(\max)}, & 1 \le \lambda_i \le \hat{s}_i^{(\max)}, \\ \lambda_i, & \lambda_i \ge \hat{s}_i^{(\max)}, \end{cases} \quad s_i^{(\min)} = \begin{cases} \hat{s}_i^{(\min)}, & 1 \ge \lambda_i \ge \hat{s}_i^{(\min)}, \\ \lambda_i, & \lambda_i \le \hat{s}_i^{(\min)}. \end{cases} \tag{83}$$

Here, the magnetic field $\boldsymbol{h}_l = h\boldsymbol{e}_2$ is considered. For this type of deformation $\zeta_1 = \zeta_3 = 0$ and $\zeta_2 = 1$. For $\theta = 0°$, $\lambda_1 = \lambda_3$ and the axial nominal stress

$$S_2 = \frac{\eta(\lambda_2, s_2^{(\max)}) f(\lambda_2) - \eta(1/\sqrt{\lambda_2}, 1/\sqrt{s_2^{(\max)}}) f(1/\sqrt{\lambda_2}) + \lambda_2 \dfrac{\partial z}{\partial \lambda_2}(\lambda_2, h) - \mu_o h^2/(2\lambda_2^2)}{\lambda_2}. \tag{84}$$

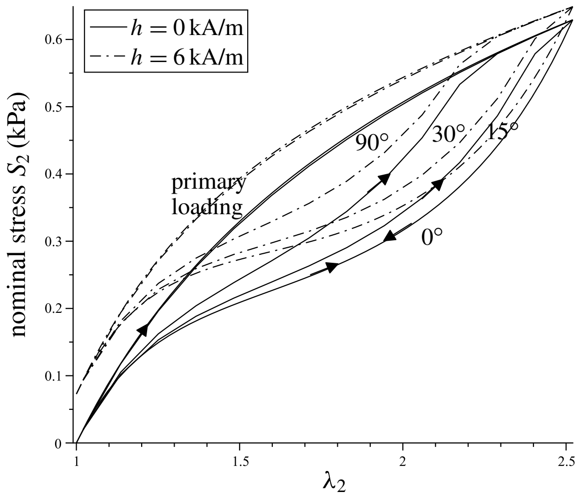

Figure 4. Induced anisotropy represented by the theoretical uniaxial stress-strain responses for the different angles between the first and second loading directions ($\boldsymbol{h}_l = h\boldsymbol{e}_2$).

In the case of when θ is nonzero, $\lambda_1 \neq \lambda_3$ in general and

$$S_2 = \frac{\eta(\lambda_2, s_2^{(\max)}) f(\lambda_2) - \eta(\lambda_3, s_3^{(\min)}) f(\lambda_3) + \lambda_2 \dfrac{\partial z}{\partial \lambda_2}(\lambda_2, h) - \mu_o h^2/(2\lambda_2^2)}{\lambda_2}. \tag{85}$$

Note that for the non-0° deformations, the value for λ_3 in (85) is obtained from λ_2 via the equation

$$\eta(\lambda_3, s_3^{(\min)}) f(\lambda_3) = \eta(1/(\lambda_2\lambda_3), s_1^{(\min)}) f(1/(\lambda_2\lambda_3)), \tag{86}$$

considering the boundary stress condition $T_{33} = -\mu_0 h^2/(2\lambda_2^2)$, the incompressibility condition $\lambda_1\lambda_2\lambda_3 = 1$ and assuming $T_{11} = T_{33}$, where T_{ij} are the components of the total stress $\boldsymbol{T}$ relative to a basis that coincide with the basis $\{\boldsymbol{e}_1, \boldsymbol{e}_2, \boldsymbol{e}_3\}$.

The anisotropic stress softening behavior for $\lambda_m = 2.5$ is clearly shown in Figure 4, where the behavior for $h = 0$ is similar to the Machado et al. [2012] experiment.

4.2. ***Anisotropy induced by a simple shear predeformation.*** The proposed model is based on direction-dependent parameters where their values depend on the principal directions of $\boldsymbol{U}$. Hence, it is important to study stress-softening behavior in a sequence of deformations when the principal directions of $\boldsymbol{U}$ change continuously. An example of such deformation is the simple shear deformations where the principal directions of $\boldsymbol{U}$ change continuously during the deformation. Shariff [2014] has studied anisotropic simple shear stress softening behavior for non-MS materials and the calculations in this section follow that paper. Consider the prestretching of a material by a simple shear deformation described by

$$\boldsymbol{U}^2(\gamma) \equiv \begin{pmatrix} 1 & \gamma & 0 \\ \gamma & 1+\gamma^2 & 0 \\ 0 & 0 & 1 \end{pmatrix}, \tag{87}$$

where $0 \le \gamma \le \gamma_m$ and γ is commonly called *the amount of shear*.

Without loss of generality, the total stress normal to the plane of shear is assumed to be zero, since incompressibility allows the superposition of an arbitrary hydrostatic stress without effecting the deformation. In view of this, the total shear stress is

$$\begin{aligned} \sigma_s &= \left[\eta(\lambda_1, \alpha_1) f(\lambda_1) - \eta(\lambda_2, \alpha_2) f(\lambda_2) + \zeta_1 \lambda_1 \frac{\partial z}{\partial \lambda_1}(\lambda_1, h) - \zeta_2 \lambda_2 \frac{\partial z}{\partial \lambda_2}(\lambda_2, h) \right] cs \\ &\qquad + \frac{2}{\lambda_1^2 - \lambda_2^2} \big[z(\lambda_1, h) - z(\lambda_2, h) \big] (\boldsymbol{e}_1 \cdot \boldsymbol{a})(\boldsymbol{e}_2 \cdot \boldsymbol{a}) \gamma cs \\ &= \Bigg[\eta(\lambda_1, \alpha_1) f(\lambda_1) - \eta(\lambda_2, \alpha_2) f(\lambda_2) \\ &\qquad + \mu_0 h^2 \left(-d_1 \zeta_1 \lambda_1 \frac{2(\lambda_1 - a) + 1}{((\lambda_1 - a)^2 + \lambda_1)^2} + d_1 \zeta_2 \lambda_2 \frac{2(\lambda_2 - a) + 1}{((\lambda_2 - a)^2 + \lambda_2)^2} + \frac{\zeta_1}{\lambda_1^2} - \frac{\zeta_2}{\lambda_2^2} \right) \Bigg] cs \\ &\qquad + \frac{2\mu_0 h^2}{\lambda_1 + \lambda_2} \left(\frac{d_1(2a - 1 - \lambda_1 - \lambda_2)}{[(\lambda_1 - a)^2 + \lambda_1][(\lambda_2 - a)^2 + \lambda_2]} - \frac{\lambda_1 + \lambda_2}{2\lambda_1 \lambda_2} \right) (\boldsymbol{e}_1 \cdot \boldsymbol{a})(\boldsymbol{e}_2 \cdot \boldsymbol{a}) \gamma cs, \end{aligned} \tag{88}$$

where [Bustamante and Shariff 2015]

$$c = \frac{1}{\sqrt{1+\lambda_1^2}}, \quad s = \frac{\lambda_1}{\sqrt{1+\lambda_1^2}}, \quad c^2 - s^2 = -\gamma cs, \tag{89}$$

$$\lambda_1 = \frac{\gamma + \sqrt{\gamma^2+4}}{2} \ge 1, \quad \lambda_2 = \frac{1}{\lambda_1} = \frac{\sqrt{\gamma^2+4} - \gamma}{2} \le 1, \quad \lambda_3 = 1. \tag{90}$$

Note that c and s in this section are different from those defined in Section 4.1.2.

4.2.1. *Simple shear of the prestretch in the primary shear direction.* Consider a simple shear deformation of the prestretched material in the same direction as the primary shear direction of the virgin material [Shariff 2014]. The components of the principal directions of $\boldsymbol{U}$ of this nonvirgin simple shear are

$$\boldsymbol{e}_1 \equiv \begin{bmatrix} c \\ s \\ 0 \end{bmatrix}, \quad \boldsymbol{e}_2 \equiv \begin{bmatrix} -s \\ c \\ 0 \end{bmatrix}, \quad \boldsymbol{e}_3 \equiv \begin{bmatrix} 0 \\ 0 \\ 1 \end{bmatrix}. \tag{91}$$

For a fixed c and s,

$$\begin{gathered} s_1^{(\max)} = \max_{0 \le \gamma \le \gamma_m} \sqrt{(\gamma s + c)^2 + s^2}, \quad s_1^{(\min)} = \min_{0 \le \gamma \le \gamma_m} \sqrt{(\gamma s + c)^2 + s^2}, \\ s_2^{(\max)} = \max_{0 \le \gamma \le \gamma_m} \sqrt{(\gamma c - s)^2 + c^2}, \quad s_2^{(\min)} = \min_{0 \le \gamma \le \gamma_m} \sqrt{(\gamma c - s)^2 + c^2}, \\ s_3^{(\max)} = s_3^{(\min)} = 1\,. \end{gathered}$$

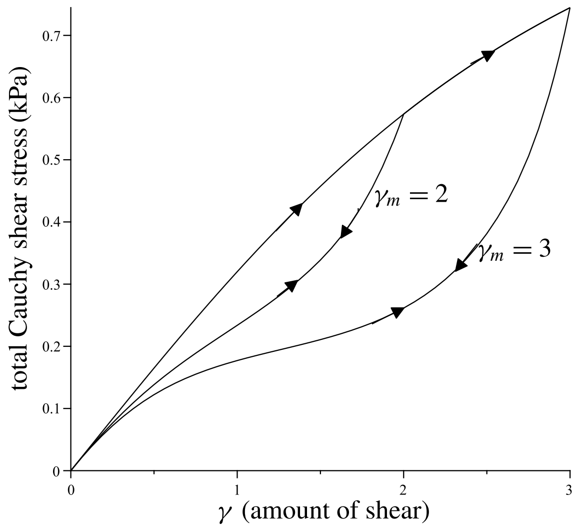

Figure 5. Simple shear loadings and unloadings in the primary shear direction.

After some manipulation, the values

$$s_1^{(\max)} = \sqrt{(\gamma_m s + c)^2 + s^2}, \quad s_1^{(\min)} = 1, \quad 0 \le \gamma \le \gamma_m, \quad \gamma_m \ge 0,$$

are obtained. For $0 \le \gamma_m \le 2$,

$$s_2^{(\max)} = 1, \quad 0 \le \gamma \le \gamma_m,$$

and for $\gamma_m > 2$

$$s_2^{(\max)} = \begin{cases} \sqrt{(\gamma_m c - s)^2 + c^2}\,, & 0 \le \gamma \le (\gamma_m^2 - 4)/(2\gamma_m), \\ 1, & (\gamma_m^2 - 4)/(2\gamma_m) < \gamma \le \gamma_m. \end{cases}$$

For $\gamma_m > 1$,

$$s_2^{(\min)} = \begin{cases} c, & 0 \le \gamma < (\gamma_m^2 - 1)/\gamma_m, \\ \sqrt{(\gamma_m c - s)^2 + c^2}, & (\gamma_m^2 - 1)/\gamma_m \le \gamma \le \gamma_m, \end{cases}$$

and for $0 \le \gamma_m \le 1$

$$s_2^{(\min)} = \sqrt{(\gamma_m c - s)^2 + c^2}, \quad 0 \le \gamma \le \gamma_m.$$

The shear stress σ_s for the primary loading is

$$\sigma_s = (f(\lambda_1) - f(\lambda_2))cs. \tag{92}$$

The shear stress for the unloading and reloading of the prestretched material is given by

$$\sigma_s = \big(\eta_1(\lambda_1, s_1^{(\max)}) f(\lambda_1) - \eta_2(\lambda_2, s_2^{(\min)}) f(\lambda_2)\big)cs. \tag{93}$$

For illustration purposes the ad-hoc values

$$a = 1.2, \quad a_1 = a_2 = 1.0\,\text{kPa}, \quad b_1 = 1.5, \quad b_2 = 0.5, \quad d_1 = -2\,\text{kPa},$$

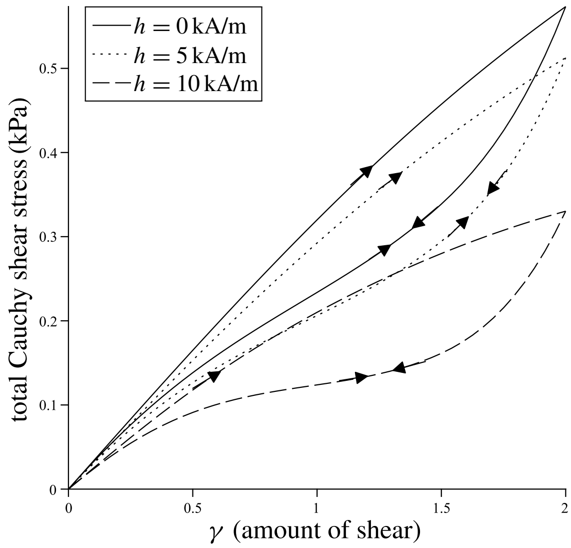

Figure 6. Simple shear loadings and unloadings in the primary shear direction in the presence of the Lagrangean magnetic field $\boldsymbol{h}_l \equiv [h, 0, 0]^T$.

are used.

Figure 5 depicts the loading and unloading curves for $\gamma_m = 2$ and $\gamma_m = 3$ when $h = 0$. It is clear from Figure 5 that the stress-deformation curves behave as expected.

Only results for constant magnetic fields $\boldsymbol{h}_l \equiv [h, 0, 0]^T$, $\boldsymbol{h}_l \equiv [0, h, 0]^T$ and $\boldsymbol{h}_l \equiv [0, 0, h]^T$ are given, taking note that the conditions in (4) are automatically satisfied. In Figure 6, the stress-strain curves for $\boldsymbol{h}_l \equiv [h, 0, 0]^T$ are depicted for $h = 0, 5, 10$. From the figure, it is found that the magnitude of the shear stress is reduced, when a magnetic field in the same direction as the shear direction is applied. The results for $\boldsymbol{h}_l \equiv [0, h, 0]^T$ are depicted in Figure 7, where in this case, a larger shear stress is required in the presence of a magnetic field. It is clear from (88), as expected, the shear stress is not affected by the magnetic field $\boldsymbol{h}_l \equiv [0, 0, h]^T$; hence, the corresponding graph will not be depicted.

In view of (88), in contrast to the simple tension case described in Section 4.1, no shear stress is required to maintain the undeformed deformation when the magnetic field $h \neq 0$ for the magnetic directions considered in this section.

4.2.2. *Simple shear of the prestretch in the opposite direction to the primary loading direction.* In this section, the prestretched material is sheared in the direction opposite to the primary direction up to $\gamma = 2$. The components of the principal eigenvectors for this opposite direction shearing are

$$\boldsymbol{e}_1 \equiv \begin{bmatrix} -c \\ s \\ 0 \end{bmatrix}, \quad \boldsymbol{e}_2 \equiv \begin{bmatrix} s \\ c \\ 0 \end{bmatrix}, \quad \boldsymbol{e}_3 \equiv \begin{bmatrix} 0 \\ 0 \\ 1 \end{bmatrix}. \tag{94}$$

Consider the extremum prestretch values

$$\hat{s}_i^{(\max)} = \max_{0 \le \gamma \le 2} \sqrt{\boldsymbol{e}_i \cdot \boldsymbol{U}^2(\gamma)\boldsymbol{e}_i}, \quad \hat{s}_i^{(\min)} = \min_{0 \le \gamma \le 2} \sqrt{\boldsymbol{e}_i \cdot \boldsymbol{U}^2(\gamma)\boldsymbol{e}_i}, \tag{95}$$

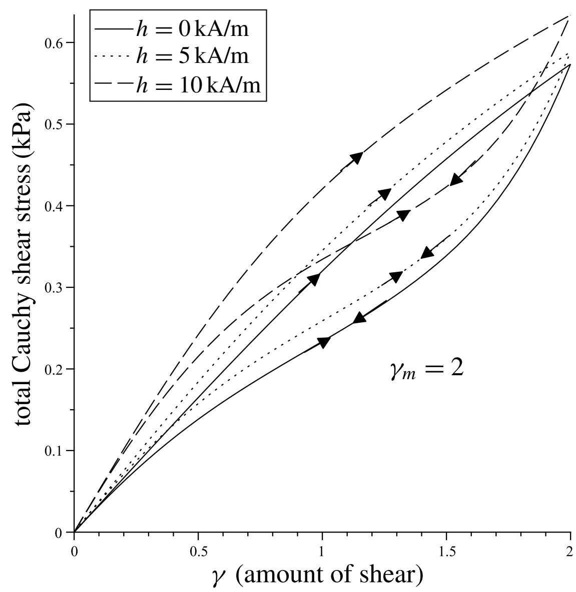

Figure 7. Simple shear loadings and unloadings in the primary shear direction in the presence of the Lagrangean magnetic field $\boldsymbol{h}_l \equiv [0, h, 0]^T$.

of the line elements of the presheared material in the $\boldsymbol{e}_i$ directions for $\gamma_m = 2$.

$$\hat{s}_1^{(\max)} = \sqrt{(2s - c)^2 + s^2}, \quad \hat{s}_1^{(\min)} = s,$$
$$\hat{s}_2^{(\max)} = \sqrt{(2c + s)^2 + c^2}, \quad \hat{s}_2^{(\min)} = 1.$$

The maximum and minimum values for the relevant principal-stretch line elements when $0 \le \gamma \le 2$ are

$$s_1^{(\max)} = \begin{cases} \hat{s}_1^{(\max)}, & 1 \le \lambda_1 \le \hat{s}_1^{(\max)}, \\ \lambda_1, & \hat{s}_1^{(\max)} \le \lambda_1 \le 1 + \sqrt{2}, \end{cases}$$
$$s_2^{(\min)} = \begin{cases} \hat{s}_2^{(\min)}, & 1 \ge \lambda_2 \ge \hat{s}_2^{(\min)}, \\ \lambda_2, & \hat{s}_2^{(\min)} \ge \lambda_2 \ge \sqrt{2} - 1, \end{cases}$$
$$s_3^{(\max)} = s_3^{(\min)} = 1.$$

4.2.3. *Simple shear of the prestretch in a direction perpendicular to the primary plane of shear.* Here, the prestretched material is sheared in a direction perpendicular to the initial plane of shear up to $\gamma = 2$. The components of the principal eigenvectors for this shearing are

$$\boldsymbol{e}_1 \equiv \begin{bmatrix} 0 \\ s \\ c \end{bmatrix}, \quad \boldsymbol{e}_2 \equiv \begin{bmatrix} 0 \\ c \\ -s \end{bmatrix}, \quad \boldsymbol{e}_3 \equiv \begin{bmatrix} 1 \\ 0 \\ 0 \end{bmatrix}. \tag{96}$$

In view of (95), the extremum values of the prestretch line elements are

$$\hat{s}_1^{(\max)} = \sqrt{4s^2 + 1}, \quad \hat{s}_1^{(\min)} = 1, \quad \hat{s}_2^{(\max)} = \sqrt{4c^2 + 1}, \quad \hat{s}_2^{(\min)} = 1.$$

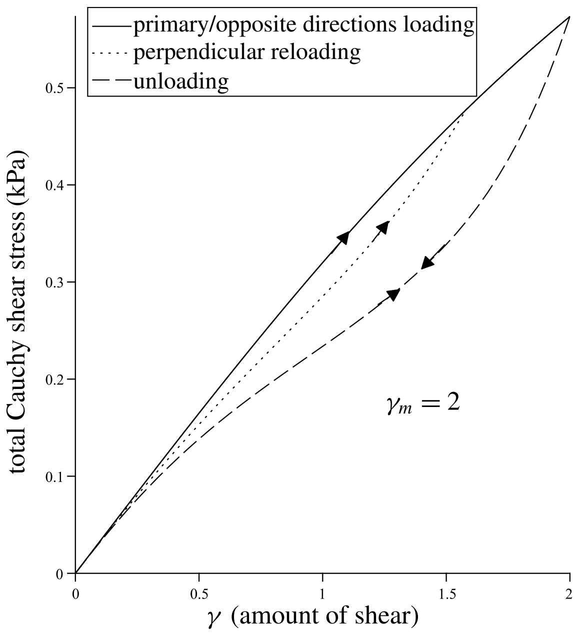

Figure 8. Simple shear in directions different from the preshear direction.

The maximum and minimum values for the relevant principal-stretch line elements for $0 \leq \gamma \leq 2$ are

$$s_1^{(\max)} = \begin{cases} \hat{s}_1^{(\max)}, & 1 \leq \lambda_1 \leq \hat{s}_1^{(\max)}, \\ \lambda_1, & \hat{s}_1^{(\max)} \leq \lambda_1 \leq 1+\sqrt{2}, \end{cases}$$

$$s_2^{(\min)} = \begin{cases} \hat{s}_2^{(\min)}, & 1 \geq \lambda_2 \geq \hat{s}_2^{(\min)}, \\ \lambda_2, & \hat{s}_2^{(\min)} \geq \lambda_2 \geq \sqrt{2}-1, \end{cases}$$

$$s_3^{(\min)} = s_3^{(\max)} = 1.$$

Figure 8 depicts, for $h = 0$, the results for various loadings given in Sections 4.2.2 and 4.2.3. The theory closely predicts the experimental results of Muhr et al. [1999], where they stated that "the softening is greatest for simple shear in the same direction, least for simple shear in the opposite direction and intermediate for shear at 90 degrees". The shear stress-strain behavior in the presence of a Lagrangean magnetic field in a direction parallel to the shear direction or perpendicular to the shear direction and parallel to the shear plane or perpendicular to the shear plane is similar to that described in 4.2.1.

5. Conclusions

The motivating key for this work is to provide a phenomenological model that could describe three dimensional anisotropic stress softening behavior (Mullins effect) of MS materials in the presence of a magnetic field, which up-to-date has not been proposed in the literature. The proposed model uses a set of spectral invariants, where each invariant has a clear physical meaning, and hence have an experimental advantage over other types of invariants with no physical interpretation such as the classical invariants by Spencer and Rivlin [1962]. Due to the absence of relevant experimental data, at the moment we are not concerned with the construction of specific forms of the functions f, η, g and q; nevertheless, the crude specific forms proposed in this paper seem to reasonably predict the anisotropic stress softening behavior of MS elastomers in the presence of a magnetic field.

Acknowledgements

The authors would like to thank the anonymous reviewers for their contribution towards the development of this paper.

References

[Bellan and Bossis 2002] C. Bellan and G. Bossis, "Field dependence of viscoelastic properties of MR elastomers", *Int. J. Modern Physics* **16** (2002), 2447–2453.

[Boczkowska and Awietjan 2012] A. Boczkowska and S. Awietjan, *Advanced elastomers: technology, properties and applications*, edited by A. Boczkowska, InTech, 2012.

[Böse et al. 2012] H. Böse, R. Rabindranath, and J. Ehrlich, "Soft magnetorheological elastomers as new actuators for valves", *J. Intell. Mater. Syst. Struct.* 23 (2012), 989–994.

[Brown 1966] W. F. Brown, *Magnetoelastic interactions*, Springer Tracts in Natural Philosophy **9**, Springer, Berlin, 1966.

[Bustamante and Shariff 2015] R. Bustamante and M. H. B. M. Shariff, "A principal axis formulation for nonlinear magnetoelastic deformations: isotropic bodies", *Eur. J. Mech. A Solids* **50** (2015), 17–27.

[Coquelle and Bossis 2006] E. Coquelle and G. Bossis, "Mullins effect in elastomers filled with particles aligned by a magnetic field", *Int. J. Solids Struct.* **43**:25–26 (2006), 7659–7672.

[Criscione 2003] J. C. Criscione, "Rivlin's representation formula is ill-conceived for the determination of response functions via biaxial testing", *J. Elasticity* **70**:1–3 (2003), 129–147.

[Danas et al. 2012] K. Danas, S. V. Kankanala, and N. Triantafyllidis, "Experiments and modeling of iron-particle-filled magnetorheological elastomers", *J. Mech. Phys. Solids* **60**:1 (2012), 120–138.

[Dorfmann and Ogden 2003] A. Dorfmann and R. W. Ogden, "Magnetoelastic modelling of elastomers", *Eur. J. Mech. A Solids* **22**:4 (2003), 497–507.

[Dorfmann and Ogden 2004a] A. Dorfmann and R. W. Ogden, "Nonlinear magnetoelastic deformations", *Q. J. Mech. Appl. Math.* **57**:4 (2004), 599–622.

[Dorfmann and Ogden 2004b] A. Dorfmann and R. W. Ogden, "Nonlinear magnetoelastic deformations of elastomers", *Acta Mech.* **167**:1–2 (2004), 13–28.

[Dorfmann and Ogden 2005] A. Dorfmann and R. W. Ogden, "Some problems in nonlinear magnetoelasticity", *Z. Angew. Math. Phys.* **56**:4 (2005), 718–745.

[Eringen and Maugin 1990] A. C. Eringen and G. A. Maugin, *Electrodynamics of continua, I*, Springer, New York, 1990.

[Farshad and Roux 2004] M. Farshad and M. L. Roux, "A new active noise abatement barrier system", *Polymer Testing* **23**:7 (2004), 855–860.

[Ghafoorianfar et al. 2013] N. Ghafoorianfar, X. Wang, and F. Gordaninejad, "On the sensing of magnetorheological elastomers", in *Sensors and smart structures technologies for civil, mechanical, and aerospace systems*, vol. 8692, edited by J. P. Lynch et al., 2013.

[Ginder et al. 2001] J. M. Ginder, W. F. Schlotter, and M. E. Nichols, "Magnetorheological elastomers in tunable vibration absorbers", pp. 103–110 in *Smart structures and materials: damping and isolation*, vol. 4331, edited by D. J. Inman, 2001.

[Govindjee and Simo 1991] S. Govindjee and J. Simo, "A micro-mechanically based continuum damage model for carbon black-filled rubbers incorporating Mullins' effect", *J. Mech. Phys. Solids* **39**:1 (1991), 87–112.

[Holzapfel and Ogden 2009] G. A. Holzapfel and R. W. Ogden, "On planar biaxial tests for anisotropic nonlinearly elastic solids: a continuum mechanical framework", *Math. Mech. Solids* **14**:5 (2009), 474–489.

[Humphrey et al. 1990] J. D. Humphrey, R. K. Strumpf, and F. C. Yin, “Determination of a constitutive relation for passive myocardium, I: A new functional form”, *J. Biomech. Eng.* **112**:3 (1990), 333–339.

[Hutter et al. 2006] K. Hutter, A. Ursescu, and A. A. F. van de Ven, *Electromagnetic field matter interactions in thermoelastic solids and viscous fluids*, Lecture Notes in Physics **710**, Springer, Berlin, 2006.

[Itskov et al. 2010] M. Itskov, A. E. Ehret, R. Kazakevičiutė-Makovska, and G. W. Weinhold, “A thermodynamically consistent phenomenological model of the anisotropic Mullins effect”, *Z. Angew. Math. Mech.* **90**:5 (2010), 370–386.

[Johnson and Beatty 1993] M. A. Johnson and M. F. Beatty, “A constitutive equation for the Mullins effect in stress controlled uniaxial extension experiments”, *Contin. Mech. Thermodyn.* **5**:4 (1993), 301–318.

[Jolly et al. 1996] M. R. Jolly, J. D. Carlson, and B. C. M. noz, “A model of the behaviour of magnetorheological materials”, *Smart Mater. and Struct.* **5**:5 (1996), 607–614.

[Kankanala and Triantafyllidis 2004] S. V. Kankanala and N. Triantafyllidis, “On finitely strained magnetorheological elastomers”, *J. Mech. Phys. Solids* **52**:12 (2004), 2869–2908.

[Kashima et al. 2012] S. Kashima, F. Miyasaka, and K. Hirata, “Novel soft actuator using magnetorheological elastomer”, *IEEE Transactions on Magnetics* **48**:4 (2012), 1649–1652.

[Kovetz 2000] A. Kovetz, *Electromagnetic theory*, Oxford University Press, Oxford, England, 2000.

[Lin and Yin 1998] D. H. Lin and F. C. Yin, “A multiaxial constitutive law for mammalian left ventricular myocardium in steady-state barium contracture or tetanus”, *J. Biomech. Eng.* **120**:4 (1998), 504–517.

[Machado et al. 2012] G. Machado, G. Chagnon, and D. Favier, “Induced anisotropy by the Mullins effect in filled silicone rubber”, *Mech. Mater.* **50** (2012), 70–80.

[Maugin 1988] G. A. Maugin, *Continuum mechanics of electromagnetic solids*, North-Holland Series in Applied Mathematics and Mechanics **33**, North-Holland Publishing Co., Amsterdam, 1988.

[Muhr et al. 1999] A. H. Muhr, J. Gough, and I. H. Gregory, “Experimental determination of model for liquid silicone rubber”, pp. 181–187 in *Constitutive models for rubber*, edited by A. Muhr and A. Dorfmann, A. A. Balkema, Rotterdam, Netherlands, 1999.

[Mullins 1947] L. Mullins, “Effect of stretching on the properties of rubber”, *J. Rubber Res.* **16** (1947), 275–289.

[Ogden and Roxburgh 1999] R. W. Ogden and D. G. Roxburgh, “A pseudo-elastic model for the Mullins effect in filled rubber”, *R. Soc. Lond. Proc. Ser. A Math. Phys. Eng. Sci.* **455**:1988 (1999), 2861–2877.

[Ogden and Steigmann 2010] R. W. Ogden and D. J. Steigmann (editors), *Mechanics and electrodynamics of magneto- and electro-elastic materials*, CISM International Centre for Mechanical Sciences **527**, Springer, Vienna, 2010.

[Pawelski 2001] H. Pawelski, “Softening behaviour of elastomeric media after loading in changing directions”, pp. 27–36 in *Constitutive models for rubber II*, edited by D. Besdo et al., A. A. Balkema, Lisse, Netherlands, 2001.

[Shariff 2000] M. H. B. M. Shariff, “Strain energy function for filled and unfilled rubberlike material”, *Rubber Chem. Technol.* **73**:1 (2000), 1–18.

[Shariff 2006] M. H. B. M. Shariff, “An anisotropic model of the Mullins effect”, *J. Eng. Math.* **56**:4 (2006), 415–435.

[Shariff 2008] M. H. B. M. Shariff, “Nonlinear transversely isotropic elastic solids: an alternative representation”, *Q. J. Mech. Appl. Math.* **61**:2 (2008), 129–149.

[Shariff 2014] M. H. B. M. Shariff, “Direction dependent orthotropic model for Mullins materials”, *Int. J. Solids Struct.* **51**:25–26 (2014), 4357–4372.

[Shariff 2016] M. H. B. M. Shariff, “Anisotropic separable free energy functions for elastic and non-elastic solids”, *Acta Mech.* (2016), 1–25.

[Simo 1987] J. C. Simo, “On a fully three-dimensional finite-strain viscoelastic damage model: formulation and computational aspects”, *Comput. Method Appl. M.* **60**:2 (1987), 153–173.

[Spencer 1971] A. J. M. Spencer, “Theory of invariants”, pp. 239–353 in *Continuum physics*, vol. 1, edited by A. C. Eringen, Academic Press, New York, 1971.

[Spencer and Rivlin 1962] A. J. M. Spencer and R. S. Rivlin, “Isotropic integrity bases for vectors and second-order tensors I”, *Arch. Rational Mech. Anal.* **9** (1962), 45–63.

[Steigmann 2004] D. J. Steigmann, "Equilibrium theory for magnetic elastomers and magnetoelastic membranes", *Int. J. Non-Linear Mech.* **39**:7 (2004), 1193–1216.

[Vu and Steinmann 2010] D. K. Vu and P. Steinmann, "Material and spatial motion problems in nonlinear electro- and magneto-elastostatics", *Math. Mech. Solids* **15**:2 (2010), 239–257.

[Zhu et al. 2012] J.-T. Zhu, Z.-D. Xu, and Y.-Q. Guo, "Magnetoviscoelasticity parametric model of an MR elastomer vibration mitigation device", *Smart Mater. Struct.* **21**:7 (2012), 075034.

Received 13 Jan 2016. Revised 14 Jun 2016. Accepted 20 Jun 2016.

M. H. B. M. SHARIFF: shariff@kustar.ac.ae
Department of Applied Mathematics and Science, Khalifa University of Science, Technology and Research, Sharjah, United Arab Emirates

ROGER BUSTAMANTE: rogbusta@ing.uchile.cl
Departamento de Ingeniería Mecánica, Universidad de Chile, Beauchef 850 Santiago Centro, Chile

JOURNAL OF MECHANICS OF MATERIALS AND STRUCTURES

msp.org/jomms

Founded by Charles R. Steele and Marie-Louise Steele

Cover photo: Wikimedia Commons

See msp.org/jomms for submission guidelines.

JoMMS (ISSN 1559-3959) at Mathematical Sciences Publishers, 798 Evans Hall #6840, c/o University of California, Berkeley, CA 94720-3840, is published in 10 issues a year. The subscription price for 2016 is US $575/year for the electronic version, and $735/year (+$60, if shipping outside the US) for print and electronic. Subscriptions, requests for back issues, and changes of address should be sent to MSP.

JoMMS peer-review and production is managed by EditFlow® from Mathematical Sciences Publishers.

PUBLISHED BY

mathematical sciences publishers

nonprofit scientific publishing

http://msp.org/

Journal of Mechanics of Materials and Structures

Volume 11, No. 5 December 2016

Interface stress of orthotropic materials with a nanodefect under antiplane shear loading
JUNHUA XIAO, CHUANFU SHI, YAOLING XU and FUCHENG ZHANG 491

Propagation of waves in masonry-like solids
MARIA GIRARDI, CRISTINA PADOVANI and DANIELE PELLEGRINI 505

Two-dimensional fretting contact of piezoelectric materials under a rigid conducting cylindrical punch
JIE SU, LIAO-LIANG KE and YUE-SHENG WANG 535

An anisotropic model for the Mullins effect in magnetoactive rubber-like materials
M. H. B. M. SHARIFF and ROGER BUSTAMANTE 559

Predictive modeling of mechanical properties of metal filled anodic aluminum oxide
VLADIMIR V. BARDUSHKIN, YULIA I. SHILYAEVA, SERGEY A. GAVRILOV, MAXIM V. SILIBIN, VICTOR B. YAKOVLEV, MIKHAIL L. ZHELUDKEVICH and NATALIA I. POPENKO 583

The hemispherical nanopit at the plane boundary of an elastic half-space subjected to statically equivalent shear tractions
CHANGWEN MI, ZHONGWEI SUN and DEMITRIS KOURIS 595

Book review: Shorr's *Thermal integrity in mechanics and engineering*
FEODOR M. BORODICH 615

1559-3959(2016)11:5;1-4